J|A|C|S ARTICLES

Published on Web 09/08/2009

Gold Nanoparticle Based Label-Free SERS Probe for Ultrasensitive and Selective Detection of Trinitrotoluene

Samuel S. R. Dasary, Anant Kumar Singh, Dulal Senapati, Hongtao Yu, and Paresh Chandra Ray*

Department of Chemistry, Jackson State University, Jackson, Mississippi 39217

Received June 22, 2009; E-mail: paresh.c.ray@jsums.edu

Abstract: TNT is one of the most commonly used nitro aromatic explosives used for landmine and military purpose. Due to the significant detrimental effects, contamination of soil and groundwater with TNT is the major concern. Driven by the need to detect trace amounts of TNT from environmental samples, this article demonstrates for the first time a highly selective and ultra sensitive, cysteine modified gold nanoparticle based label-free surface enhanced Raman spectroscopy (SERS) probe, for TNT recognition in 2 pico molar (pM) level in aqueous solution. Due to the formation of Meisenheimer complex between TNT and cysteine, gold nanoparticles undergo aggregation in the presence of TNT via electrostatic interaction between Meisenheimer complex bound gold nanoparticle and cysteine modified gold nanoparticle. As a result, it formed several hot spots and provided a significant enhancement of the Raman signal intensity by 9 orders of magnitude through electromagnetic field enhancements. A detailed mechanism for termendous SERS intensity change has been discussed. Our experimental results show that TNT can be detected quickly and accurately without any dye tagging in lower pM level with excellent discrimination against other nitro compounds and heavy metals.

Introduction

2,4,6-Trinitrotoluene (TNT) is one of the most commonly used explosives in the preparation of landmines for military and terrorist activities.[1,2] Contamination of soil and groundwater with TNT is the major concern because of its biological persistence, toxicity and mutagenicity.[3,4] TNT can absorb through the skin and people who are exposed to TNT over a prolonged period tend to experience anemia and abnormal liver functions. Recently, global security concerns have also dictated a need for the detection of hidden explosive devices in war zones and transportation hubs. As a result, it is important to develop highly sensitive, cost-effective probe that can provide real-time determination of TNT level in the environment. Current technology for the detection of TNT is less sensitive and usually time-consuming with the employment of cumbersome and expensive gas chromatography coupled to a mass spectrometer, ion mobility spectrometry, and neutron activation analysis.[5,6] They are too slow from the perspective of day-to-day life needs for on-the-spot detection. To address the growing market needs in the 21st century, future devices must link high performance, with speed, simplicity and low cost.[5−8] As a result, the development of ultrasensitive assays for the real-time detection of TNT has attracted considerable research efforts in recent years.[5−18] Different sensors for analyzing TNT have been reported in last 10 years, which includes optical sensors such as, QD, silica nanoparticle and organic dyes based fluorescence resonance energy transfer (FRET), conjugated polymer based single and mutiphoton sensor. But these assays identify the TNT analyte through a covalently linked label such as a fluorescence or luminescence tag. Necessity of tagging makes it difficult to

(1) Smith, K. D.; McCord, B. R.; MacCrehan, W. A.; Mount, K.; Rowe, W. F. *J. Forensic Sci.* **1999**, *44*, 789–794.
(2) Charles, P. T.; Dingle, B. M.; Van Bergen, S.; Gauger, P. R.; Patterson, C. H.; Kusterbeck, A. W. *Field Anal. Chem. Technol.* **2001**, *5*, 272–280.
(3) Dillewijn, P. V.; Couselo, J. L.; Corredoira, E.; Delgado, A.; Wittich, R. M.; Ballester, A.; Ramos, J. L. *Environ. Sci. Technol.* **2008**, *42*, 7405–7410.
(4) Hawari, J.; Beaudet, S.; Halasz, A.; Thiboutot, S.; Ampleman, G. *Appl. Microbiol. Biotechnol.* **2000**, *54*, 605–618.
(5) Swager, T. M. *Acc. Chem. Res.* **1998**, *31*, 201–20.
(6) McQuade, D. T.; Pullen, A. E.; Swager, T. M. *Chem. Rev.* **2000**, *100*, 2537–2574.
(7) Sohn, H.; Sailor, M. J.; Magde, D.; Trogler, W. C. *J. Am. Chem. Soc.* **2003**, *125*, 3821–3830.
(8) Riskin, M.; Tel-Vered, R.; Lioubashevski, O.; Willner, I. J. *Am. Chem. Soc.* **2009**, *131*, 7368–7378.
(9) Riskin, M.; Tel-Vered, R.; Bourenko, T.; Granot, E.; Willner, I. *J. Am. Chem. Soc.* **2008**, *130*, 9726–9733.
(10) Goldman, E. R.; Medintz, I. L.; Whitley, J. L.; Hayhurst, A.; Clapp, A. R.; Uyeda, T. H.; Deschamps, J. R.; Lassman, M. E.; Mattoussi, H. *J. Am. Chem. Soc.* **2005**, *127*, 6744–6751.
(11) Forzani, E. R.; Lu, D.; Leright, M. J.; Aguilar, D. A.; Tsow, F.; Iglesias, R. A.; Zhang, Q.; Lu, J.; Li, J.; Tao, N. *J. Am. Chem. Soc.* **2009**, *131*, 1390–1391.
(12) Andrew, T. L.; Swager, T. M. *J. Am. Chem. Soc.* **2007**, *129*, 7254–7255.
(13) Narayanan, A.; Varnavski, O. P.; Swager, T. M.; Goodson, T., III *J. Phys. Chem. C* **2008**, *112*, 881–884.
(14) Jiang, Y.; Zhao, H.; Zhue, N.; Lin, Y.; Yu, P.; Mao, L. *Angew. Chem., Int. Ed.* **2008**, *47*, 8601–8604.
(15) Freeman, R.; Willner, I. *Nano Lett.* **2009**, *9*, 322–326.
(16) Trammell, S. A.; Zeinali, M.; Melde, B. J.; Charles, P. T.; Velez, F. L.; Dinderman, M. A.; Kusterbeck, A.; Markowitz, M. A. *Anal. Chem.* **2008**, *80*, 4627–4633.
(17) Cerruti, M.; Jaworski, J.; Raorane, D.; Zueger, C.; Varadarajan, J.; Carraro, C.; Lee, S. K.; Maboudian, R.; Majumdar, A. *Anal. Chem.* **2009**, *81*, 4192–4199.
(18) Gao, D.; Wang, Z.; Liu, B.; Ni, L.; Wu, M.; Zhang, Z. *Anal. Chem.* **2008**, *80*, 8545–8553.

10.1021/ja905134d CCC: $40.75

use the FRET technique as biosensors for real life. Driven by the need, in this article, we demonstrate that cysteine modified gold nanoparticle based surface enhanced Raman scattering (SERS) probe can be used for label-free detection of TNT, with excellent detection limit (50 pico-molar) and selectivity over DNT and other nitrocompounds.

In the last 15 years, the field of biological and chemical sensors using nanomaterial has witnessed an explosion due to the unique optical properties of noble metal nanostructures.[19−29] The collective oscillation of surface electrons on nanostructured materials has been leveraged for the amplification of optical processes in Raman scattering.[30−37] The phenomenon of SERS is generally explained by a combination of an electromagnetic (EM) mechanism describing the surface electron movement in the substrate and a chemical mechanism related to charge transfer (CT) between the substrate and the analyte molecules.[36−46] The possibility of observing Raman signals, which are normally very weak, with enhancements of the order of 10^8-10^{14} and the unique ability to obtain molecular recognition of an analyte at very low concentrations in aqueous environment allow SERS to be unique for ultrasensitive biological and chemical analysis and environmental sensing.[34−47] In addition to sensitivity, another important feature of SERS is the level of detection specificity that can be achieved by controlling the chemistry around the metal surface. By incorporating a specific chemical moiety on the SERS surface, one can target the detection of a single species present in a complex sample mixture at nano to femto molar level without having to physically separate out interfering species.[36−49] Very high selectivity and sensitivity offered by SERS, along with the highly informative spectra characteristics of Raman spectroscopy, allows SERS-based method a feasible alternative to more commonly used optical sensing methods. Remote sensing using SERS has been demonstrated at distances of up to 10 m using fiber-optically coupled probe coupled with telephoto lens.[48,49] Using those unique SERS properties, we report for the first time cysteine modified gold nanoparticle based miniaturized, inexpensive ultrasensitive surface enhanced Raman scattering (SERS) probe, for highly sensitive and selective screening of TNT from aqueous solution. This nanotechnology based method could be adapted for the detection of a wide variety of explosives used as bioterrorism agents and for military purpose. Our results demonstrate the potential for a broad application of this type of nanotechnology in practical applications in various explosive detection systems.

Materials and Experiments

Hydrogen tetrachloroaurate ($HAuCl_4.3H_2O$), $NaBH_4$, sodium citrate, L-cysteine, 2,6-dinitrotoluene, nitrophenol, acetontrile and ethanol were purchased from Sigma-Aldrich and used without further purification. 2,4,6-Trinitrotoluene was provided by ERDC, Vicksburg, MS.

Gold Nanoparticle Synthesis. Gold nanoparticles of different sizes and shapes were synthesized by controlling the ratio of $HAuCl_4$, $3H_2O$ and sodium citrate concentration as we reported recently.[21−24,46] $HAuCl_4$ trihydrate (1.8 mL, 0.01 M) in water and 0.5 mL of 0.01 M sodium citrate in water were added to 40 mL of deionized H_2O and stirred. Next, 0.12 mL of freshly prepared 0.1 M $NaBH_4$ was added and the solution color changed from colorless to orange. Stirring was stopped and the solution was left undisturbed for 2 h. The resulting spherical gold nanoparticles were 30 nm in diameter. JEM-2100F transmission electron microscope (TEM) and UV−visible absorption spectrum were used to characterize the nanoparticles. The particle concentration was measured by UV−visible spectroscopy using the molar extinction coefficients at the wavelength of the maximum absorption of each gold colloid as reported recently[21−24,46] [$\varepsilon_{(30)\ 530\ nm} = 3.0 \times 10^9\ cm^{-1}\ M^{-1}$].

Gold Nanoparticle Surface Modification. For selective detection of TNT, we have modified the gold nanoparticle surface by cysteine. 9:1 volume ratio of freshly prepared AuNPs (0.5nM) and cysteine (10^{-6} M) were mixed by stirring for 12hrs. Excess cysteine was removed by centrifugation at 8000 rpm for several minutes. By using UV−vis absorption spectra we estimated average 8−10 cystein/gold nanoparticle.

Portable Surface Enhanced Raman Spectroscopy (SERS) Probe. The schematic presentation of the portable sensor configuration is shown in the Figure 1. We have used a continuous wavelength DPSS laser from laser glow technology (LUD-670) operating at 670 nm, as an excitation light source. This light source has a capability that can minimize whole sensor configuration. We have used InPhotonics 670 nm Raman fiber optic probe for excitation and data collection. It is a combination of 90 μm excitation fiber and 200 μm collection fiber with filtering and steering micro-optics. One drop of TNT solution was kept on glass slide and the sample was excited using $\sim$ 2 mW 670 nm light. We

(19) Stewart, M. E.; Anderton, C. R.; Thompson, L. B.; Maria, J.; Gray, S. K.; Rogers, J. A.; Nuzzo, R. G. *Chem. Rev.* **2008**, *108*, 494–521.
(20) Ni, W.; Yang, Z.; Chen, H.; Li, L.; Wang, J. *J. Am. Chem. Soc.* **2008**, *130*, 6692–6693.
(21) Griffin, J.; Singh, A. K.; Senapati, D.; Rhodes, P.; Mitchell, K.; Robinson, B.; Yu, E.; Ray, P. C. *Chem.—Eur. J.* **2009**, *15*, 342–351.
(22) Darbha, G. K.; Singh, A. K.; Rai, U. S.; Yu, E.; Yu, H.; Ray, P. C. *J. Am. Chem. Soc.* **2008**, *130*, 8038.
(23) Ray, P. C. *Angew. Chem. Int. Ed* **2006**, *45*, 1151–1154.
(24) Griffin, J.; Singh, A. K.; Senapati, D.; Lee, E.; Gaylor, K.; Jones-Boone, J.; Ray, P. C. *Small* **2009**, *5*, 839–845.
(25) Alivisatos, P. **2004**, *22*, 47–52.
(26) Donath, E. *Nat. Nanotech.* **2009**, *4*, 215–216.
(27) Huang, X.; El-Sayed, I. H.; Qian, W.; El-Sayed, M. A. *J. Am. Chem. Soc.* **2006**, *128*, 2115–2120.
(28) Dubertret, B.; Calame, M.; Libchaber, C. *Nat. Biotechnol.* **2001**, *19*, 365–370.
(29) Rosi, N. L.; Mirkin, C. A. *Chem. Rev* **2005**, *105*, 1547.
(30) Steinfeld, J. I.; Wormhoudt, J. *Annu. Rev. Phys. Chem.* **1998**, *49*, 203.
(31) DiLella, D. P.; Moskovits, M. *J. Phys. Chem.* **1981**, *85*, 2042–2046.
(32) Laurence, T. A.; Braun, G.; Talley, C.; Schwartzberg, A.; Moskovits, M.; Reich, N.; Huser, T. *J. Am. Chem. Soc.* **2009**, *131*, 162–169.
(33) Camden, J. P.; Dieringer, J. A.; Zhao, J.; Van Duyne, R. P. *Acc. Chem. Res.* **2008**, *41*, 1653–1661.
(34) Moskovits, M. *Rev. Mod. Phys.* **1985**, *57*, 783–826.
(35) Kneipp, K.; Yang, W.; Kneipp, H.; Perelman, L. T.; Itzkan, I.; Dasari, R. R.; Feld, M. S. *Phys. Rev. Lett.* **1997**, *78*, 1667–1670.
(36) Nie, S.; Emory, S. R. *Science* **1997**, *275*, 1102–1106.
(37) Camden, J. A.; Dieringer, J. A.; Wang, Y.; Masiello, D. J.; Marks, L. D.; Schatz, G. C.; Van Duyne, R. P. *J. Am. Chem. Soc.* **2008**, *130*, 12616–12617.
(38) Dieringer, J. A.; Lettan, R. B., II; Scheidt, K. A.; Van Duyne, R. P. *J. Am. Chem. Soc.* **2007**, *129*, 16249–16256.
(39) Bell, S. E. J.; Sirimuthu, N. M. S. *J. Am. Chem. Soc.* **2006**, *128*, 15580–15581.
(40) Cao, Y. C.; Jin, R.; Mirkin, C. A. *Science* **2002**, *297*, 1536–1541.
(41) Camden, J. P.; Dieringer, J. A.; Wang, Y.; Masaiello, D. J.; Marks, L. D.; Schatz, G. C.; Van Duyne, R. P. *J. Am. Chem. Soc.* **2008**, *130*, 12616–12617.
(42) Barhoumi, A.; Zhang, D.; Tam, F.; Halas, N. J. *J. Am. Chem. Soc.* **2008**, *130*, 5523–5529.
(43) Qian, X.; Li, J.; Shuming, N. *J. Am. Chem. Soc.* **2009**, *131*, 7540–7541.
(44) Graham, D.; Thimpson, D. G.; Smith, W. E.; Faulds, K. *Nat. Nanotechnol.* **2008**, *3*, 548–551.
(45) Brus, L. *Acc. Chem. Res.* **2008**, *41*, 1742.
(46) Tiwari, V.; Tovmachenko, O.; Darbha, G. K.; Hardy, W.; Singh, J. P.; Ray, P. C. *Chem. Phys. Lett.* **2007**, *446*, 77–82.
(47) Jerez-Rozo, J. I.; Primera-Pedrozo, O. M.; Barreto-Caban, M. A.; Hernandez-Rivera, S. P. *Sensors J., IEEE* **2008**, *8*, 974–982.
(48) Hutchison, J. A.; Centeno, S. P.; Odaka, H.; Fukumura, H.; Hofkens, J.; Hiroshi, U.-I. *Nano Lett.* **2009**, *9*, 995–1001.
(49) Alarie, J. P.; Stokes, D. L.; Sutherland, W. S.; Edwards, A. C.; Vo-Dinh, T. *Appl. Spectrosc.* **1992**, *46*, 1608–1612.

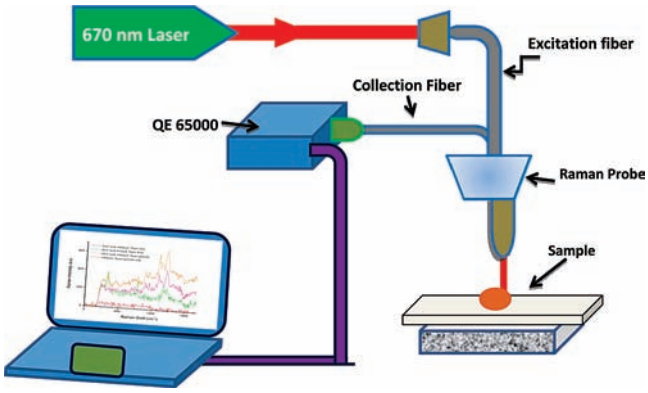

Figure 1. Schematic representation of our portable SERS probe, used for TNT detection.

have used miniaturized QE65000 Scientific-grade Spectrometer from Ocean Optics as a Raman detector. The spectral response range of this mini Raman spectrometer is 220−3600 cm^{-1}. It is equipped with TE cooled 2048 pixel CCD and interfaced to computer via a USB port. The Hamamatsu FFT-CCD detector used in the QE65000 provides 90% quantum efficiency with high signal-to-noise and rapid signal processing speed as well as remarkable sensitivity for low-light level applications. Raman spectrum was collected with Ocean Optics data acquisition SpectraSuite spectroscopy software.

Results and Discussion

Our detection is based on the fact that in the presence of TNT, cysteine-conjugated gold nanoparticles forms Meisenheimer complex (as shown in Figure 2A) and due to electrostatic interaction between gold nanoparticle bound Meisenheimer complex and cysteine bound gold nanoparticle, they undergo aggregation (as shown in Figure 2B).

As a result, it formed several hot spots and provided a significant enhancement of the Raman signal intensity by several orders of magnitude (10^9) through electromagnetic field enhancements. In our study, we have used cysteine as the primary amine as well as stabilizer for the gold nanoparticles. After the addition of cysteine to freshly prepared citrate-stabilized gold nanoparticles, the nanosurfaces were modified by cysteine through the Au−S covalent bond (as shown in Figure 2A). The addition of cysteine does not change the color and absorption spectrum of the gold nanoparticles remains the same, which indicates that there is no aggregation when 9:1 volume ratio of freshly prepared AuNPs (0.5 nM) and cysteine (10^{-6} M) was stirred. TEM image of cysteine modified gold nanoparticle, as shown in Figure 2E, also confirmed it. Now when we added TNT to cysteine modified gold nanoparticle, it undergoes aggregation (as shown in Figure 2F). TNT is known to form Meisenheimer complex with cysteine.[50,51] Recently Fant et al.[50,51] has shown using ^{13}C NMR spectroscopy that TNT chemically forms a Meisenheimer complex with cysteine. Meisenheimer complexes (as shown in Figure 3A) are σ-complexes formed by covalent addition of nucleophiles to a ring carbon atom of electron-deficient aromatic substrates. Since TNT is typically electron-deficient due to the strong electron-withdrawing effect of the nitro group, TNT is able to form Meisenheimer complexes even in the gas phase.[51] When we added 10 mM cysteine and 1 mM TNT, using condition similar to NMR experiments that has been performed by Fant et. al,[50] the color of TNT solution become red (as shown in Figure 3B), which indicates the formation of Meisenheimer complex. The UV−vis spectra (as shown in Figure 3C) of the complex shows two new absorption bands appears at 525 and 630 nm, due to the formation of Meisenheimer complex. We found that by varying the concentration of TNT (25 μM to 1 mM), one can tune the visible absorption band intensity of Meisenheimer complex. This allows us to find the association constant between TNT and cysteine by monitoring the absorption band of Meisenheimer complex at different concentrations of TNT. Our measured association constant was 9.4×10^4, which is quite similar to the reported association constant for other amines.[52]

To understand the structure of Meisenheimer complex, we also performed normal Raman spectra of 10 mM TNT and that of Meisenheimer complex (as shown in Figure 3D). Comparison of both spectra clearly shows a strong broadband appears around 2900 cm^{-1} for Meisenheimer complex and it is due to the NH_2^+ symmetric stretch, C−H stretching and CH_2 asymmetric stretching. Figure 2D shows the SERS spectra of 50 nM to 800 pM TNT, upon addition into cysteine modified gold nanoparticle. The SERS spectrum (as shown in Figure 2D) exhibits several prominent TNT peaks. Peak at 1615 cm^{-1} is due to the C═C aromatic stretching vibration. Strong Raman band at 1360.1 cm^{-1} is due to the NO_2 symmetric stretching vibration and weak band at 1533.9 cm^{-1} is due to the NO_2 asymmetric stretching vibration. Other observed Raman bands such as 1210.5 cm^{-1} is due to C_6H_2−C vibration, 1026 cm^{-1} is due to CH_3 deformation, 940 cm^{-1} and 909 cm^{-1} are due to C−N stretching vibration and 790 cm^{-1} is due to C−H out-of-plane bend. All of them are due to TNT vibration.[53,54]

In our SERS spectra (Figure 2D), we also noted a clearly broad Raman band around 2900 cm^{-1}, which indicates the formation of Meisenheimer complex (as shown in Figure 2A). So our SERS spectra also clearly show the formation of small amount of Meisenheimer complex even at the nM TNT concentration. Using our measured association constant, we calculated that the amount of Meisenheimer complex would be ~0.1 nM, when 10 nM TNT is mixed with 100 nM cysteine modified gold nanoparticle. Since TNT concentration (nM) is 100 times more than the Meisenheimer complex, the SERS spectra shows strong TNT vibration and weak vibrational band from Meisenheimer complex.

Our pH measurement shows that after mixing of TNT with cysteine modified gold nanoparticle, pH of the solution becomes 6.5. In this pH, cysteine remains in Zwitterionic form, as shown in Figure 2A and B. In this situation, gold nanoparticle attached with Meisenheimer complex can undergo aggregation with cysteine modified gold nanoparticle via electrostatic interaction and hydrogen bonding (as shown in Figure 2B). We believe that Meisenheimer complex formation and this electrostatic interaction help cysteine modified gold nanoparticles to aggregate in the presence of TNT. Cysteine modified gold nanoparticle, is known to aggregate through electrostatic and hydrogen bonding interaction, at higher concentrations (10^{-4} M cysteine or above).[55,56] Since we have used 10^{-7} M of

(50) Fant, F.; De Sloovere, A.; Matthijsen, K.; Marle, C.; Fantroussi El, S.; Verstraete, W. *Environ. Pollut.* **2001**, *503*, 507.
(51) Jehuda, Y.; Johonson, V. J.; Bernier, R. U.; Yost, A. R.; Mayfield, T. H.; Mahone, W. C.; Vorbeck, C. *J. Mass Spect.* **2005**, *30*, 715–722.
(52) Sharma, S. P.; Lahiri, S. C. *Spectra. Chem. Acta.* **2008**, *70*, 144–153.
(53) Gupta, N.; Dahmani, R. *Spectra. Chem. Acta* **2000**, *56*, 1453–1456.
(54) Kneipp, K.; Wang, Y.; Dasari, R. R.; Feld, M. S.; Gilbert, B. D.; Janni, J.; Steinfeld, J. I. *Spectra. Chim. Acta* **1995**, *51*, 2171–2175.
(55) Zhong, Z.; Subramanian, A. S.; Highfield, J.; Carpenter, K.; Gedanken, A. *Chem.—Eur. J.* **2005**, *11*, 1473–1478.

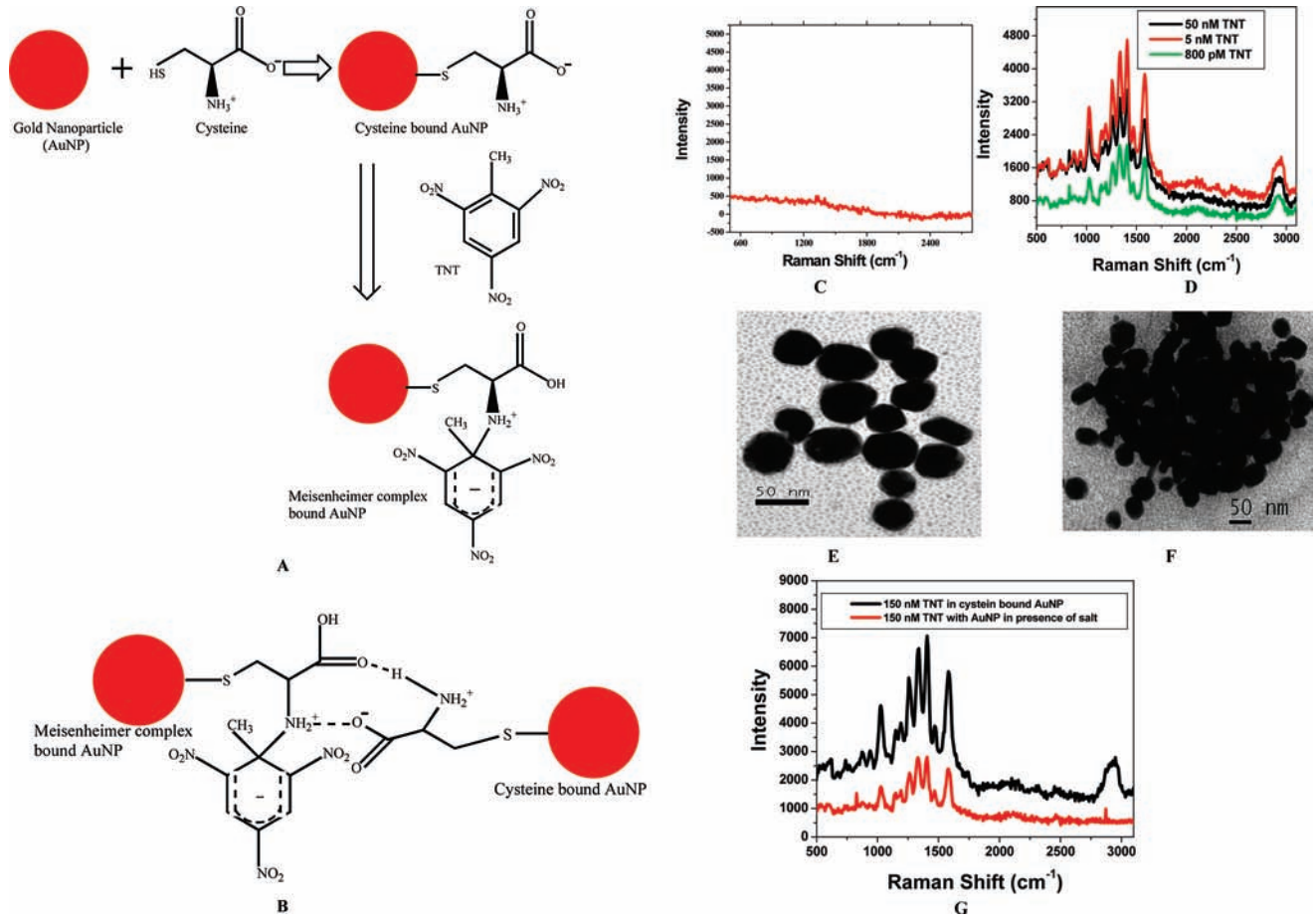

Figure 2. (A) Schematic representation of the formation of Meisenheimer complex between cysteine modified gold nanoparticle and TNT. (B) Schematic representation for the possible cross-linking between gold nanoparticle bound Meisenheimer complex with gold nanoparticle bound cysteine, (C) SERS spectra from gold nanoparticle + TNT (50×10^{-7} M), (D) SERS spectra from cysteine modified gold nanoparticle + TNT (50 nM − 800 pM TNT), (E) TEM image of cysteine modified gold nanoparticle, (F) TEM image demonstrating aggregation of gold nanoparticle in the presence of TNT, (G) SERS spectra from gold nanoparticle + TNT (150×10^{-9} M) in presence of 0.2 M NaCl and SERS spectra from cysteine modified gold nanoparticle + TNT (150 nM).

cysteine, we have not observed any aggregation, when we added cysteine to gold nanoparticle solution, as shown in Figure 2E. But in the presence of TNT, due to the formation of Meisenheimer complex, it undergoes aggregation though the concentration of Meisenheimer complex is very low. This indicates that Meisenheimer complex bound gold nanoparticle has strong ability to form aggregate with normal cysteine bound gold nanoparticle in comparison to the formation of aggregate by cysteine bound gold nanoparticle with itself. Figure 2E and F shows the TEM image of cysteine modified gold nanoparticle in the presence and the absence of TNT. Aggregation in the presence of TNT ions results in both a substantial shift in the plasmon band energy to longer wavelength and a red-to-blue color change (as shown in Figure 4A and B). The largest Raman scattering enhancements, even single molecule SERS, have been described for molecules residing in the fractal space between aggregated colloidal nanoparticles.[36−47] This is attributed to plasmonic coupling between nanoparticles in close proximity, which results in huge local electromagnetic field enhancements in these confined junctions or SERS "hot spots".[36−47] So our data clearly show that TNT helps to generate hot spots through aggregation by cysteine modified gold nanoparticle surface and as result, we have noted about 9 orders of magnitude enhancement of Raman signal (as shown in Figure 2C and D). To understand whether aggregation is necessary to observe strong SERS spectra from nM region TNT, we also did gold nanoparticle adsorbed TNT SERS experiment, in the presence of 0.1 M NaCl. We and other groups[20−27] have reported in several publications that sodium chloride helps gold nanoparticle to aggregate. As shown in Figure 2G, the SERS spectra looks very similar for 150 nM TNT adsorbed gold nanoparticle in the presence of salt and the same concentration of TNT in the presence of cysteine bound gold nanoparticle. Only exception is the presence of broadband around 2900 cm^{-1}, due to the formation of Meisenheimer complex in the presence cysteine modified gold nanoparticle. Since after aggregation, the plasmon band moves from visible to near-infrared region, partial SERS enhancements can be due to the better overlap between nano aggregate plasmon band with the excitation source. Due to the resonance, in the case of nano aggregate, EM contribution can be by 2−3 orders of magnitude higher. Our time dependent SERS data indicate that this nanobased SERS assay is rapid, takes less than 10 min from TNT binding to detection and analysis, as well as it is highly convenient. When we added TNT to pure gold nanoparticle solution, we have not observed any color change (as shown in Figure 3A) and also our TEM experiment shows that there is no aggregation. As a result, hot spot has not been generated and we have not observed any TNT

(56) Lu, C.; Zu, Y. *Chem. Comm.* **2007**, 3871–3973.

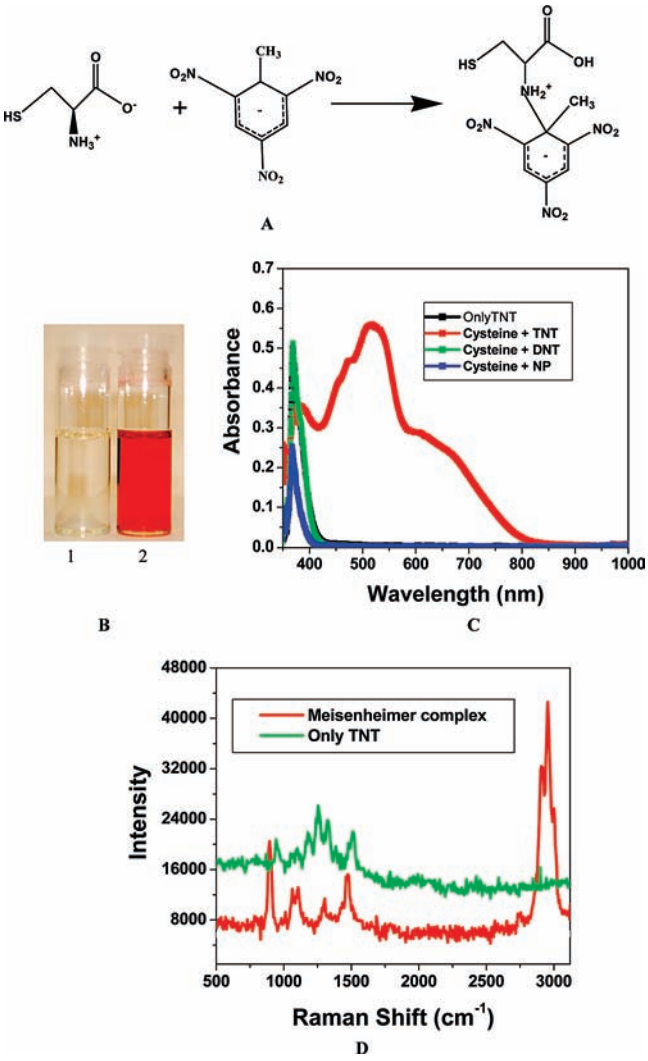

Figure 3. (A) Schematic representation of the formation of Meisenheimer complex between cysteine and TNT, (B) Photograph showing how TNT changes the color when it forms Meisenheimer complex with cysteine (10 mM cysteine + 1 mM TNT), (1) 1 mM only TNT, (2) Meisenheimer complex after addition of 10 mM cysteine in 1 mM TNT), (C) absorption spectra demonstrating new peaks at 520 and 630 nm due to the formation of Meisenheimer complex in presence of 1 mM TNT, we have not observed any visible band between 450 to 800 nm in presence of 100 mM DNT or NP. (D) Normal Raman spectra from 10 mM TNT and Meisenheimer complex.

SERS signal from TNT adsorbed gold nanoparticle surface, as shown in Figure 2C. So our result clearly shows that amine ligand modified gold nanoparticle is a must to generate hot spot in the presence of TNT.

The Raman enhancement, G, is measured experimentally by direct comparison as shown below,

$$G = [I_{SERS}]/[I_{Raman}] \times [M_{bulk}]/[M_{ads}]$$

where M_{bulk} is the number of molecules sampled in the bulk, M_{ads} is the number of molecules adsorbed and sampled on the SERS-active substrate, I_{SERS} is the intensity of a vibrational mode in the surface-enhanced spectrum, and I_{Raman} is the intensity of the same mode in the Raman spectrum. All spectra are normalized for integration time. An enhancement factor estimated from the SERS signal and general Raman signal ratio for 1360 cm^{-1} band (NO_2 symmetric stretching vibration) is approximately 1×10^9. No significant changes in Raman

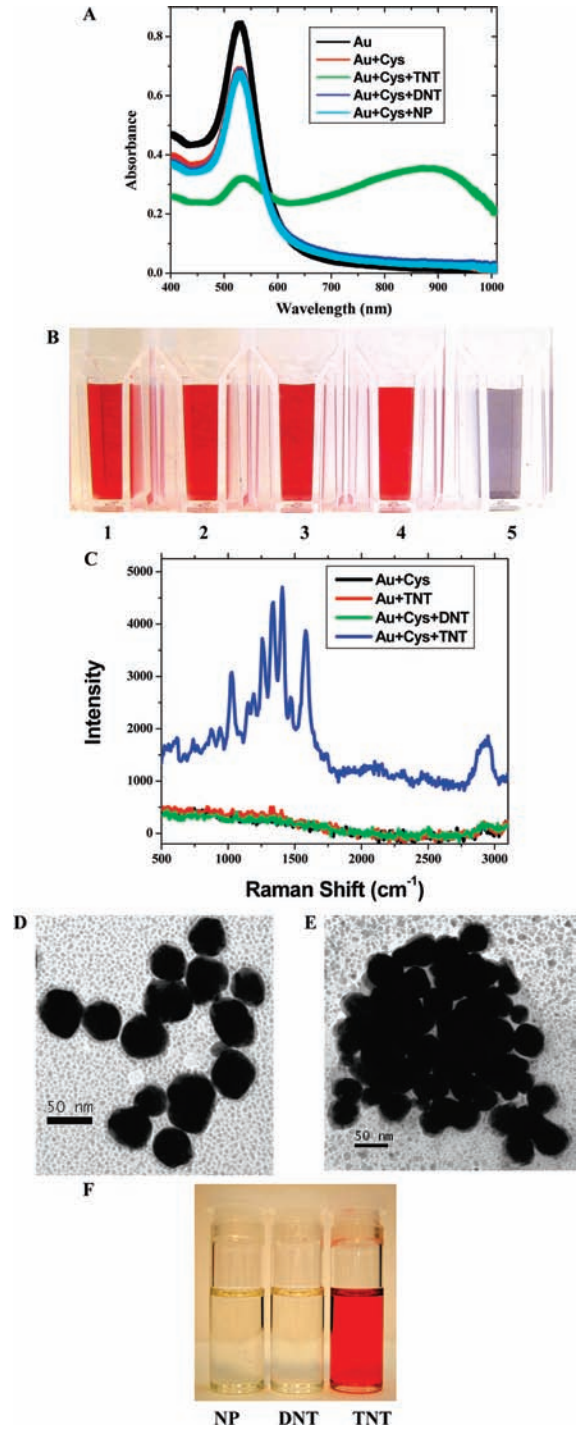

Figure 4. (A) Absorption spectral changes of cysteine modified gold nanoparticle in the presence of TNT. Absorption spectra remain same in the presence of DNT or nitro phenol (NP). (B) Photograph showing colorimetric image of gold nanoparticle in the presence of (1) only gold nanoparticle, (2) cysteine modification, (3) cysteine modified gold nanoparticle + DNT (50×10^{-6} M), (4) cysteine modified gold nanoparticle + NP (50×10^{-6} M), (5) cysteine modified gold nanoparticle + TNT ((50×10^{-9} M). Color remains same in the presence of DNT or nitro phenol. (C) Plot demonstrating SERS spectra in the presence of TNT, DNT and NP, (D) TEM image of cysteine modified gold nanoparticle in the presence of DNT ((50×10^{-6} M), (E) TEM image of cysteine modified gold nanoparticle in the presence of TNT (50×10^{-9} M). (F) Photograph showing formation of Meisenheimer complex in presence of TNT (500 μM) only. DNT and NP do not form Meisenheimer complex even at 100 mM concentration.

frequencies are observed in comparison with the corresponding SERS and Raman bands.

To understand whether our assay is highly selective, we have also performed how SERS intensity changes upon addition of 2,4 -dinitrotoluene (DNT), nitrobenzene and nitrophenol. Figure 4C shows the SERS response of our probe in the presence of various nitro-compounds. Our result clearly shows no Raman signal from DNT and nitrophenol, which shows excellent selectivity of our probe over DNT, nitro-benzene and nitro phenol. Figure 4A shows the absorption change, Figure 4B demonstrates the colorimetric response and Figure 4D,E shows the TEM images in the presence of various nitro aromatic compounds.

Our absorption and colorimetric study clearly demonstrates that cysteine modified gold nanoparticle does not undergo aggregation in the presence of DNT and other nitro compounds, which is also confirmed by TEM experiments. To understand the selectivity over DNT and nitro compounds, we examined whether cysteine forms Meisenheimer complex in the presence of DNT and nitro phenol. As shown in Figure 4F, we have not observed red color Meisenheimer complex even at the concentration of 100 mM DNT and NP, where as we see clearly strong red color Meisenheimer complex in the presence of 500 μM TNT. Even our absorption spectra measurements (as shown in Figure 3C) clearly show that there are no visible bands between 450 and 800 nm in the presence of DNT or NP, whereas we observe a very strong absorption bands with peaks at 525 and 630 nm in the presence of TNT, which is due to the formation of Meisenheimer complex. So our experimental results clearly demonstrate that DNT and NP are not able to form Meisenheimer complex, even at 100 mM concentration, whereas TNT can form Meisenheimer complex even at the concentration of 500 μM. In the case of DNT, it is most probably possible to deprotonate at the methyl group. But due to the lack of -NO_2 group in fourth position of the benzene ring, partial negative charge may not be distributed throughout the DNT molecular ring. Due to the lack of enough anionic charge, DNT may not form Meisenheimer complex and as a result, aggregation of cysteine modified gold nanoparticles is prevented. The same phenomenon can explain why nitro phenol is not forming aggregated cysteine modified gold nanoparticles. So our result clearly shows excellent selectivity of our probe over DNT and nitro phenol.

For real life application, in environmental sample, there can be several impurities due to the heavy metal ions. As a result, we also tested the selectivity of our SERS probe in the presence of alkali, alkaline earth (Li^+, Na^+, K^+, Mg^{2+}, Ca^{2+}) and transition heavy metal ions (Pb^{2+}, Pb^+, Mn^{2+}, Fe^{2+}, Cu^{2+}, Ni^{2+}, Zn^{2+}, Cd^{2+}). Since aggregation is necessary for hot spot formation, we have measured the aggregate absorbance between (630−900) nm, upon addition of other impurities. Figure 5 shows the aggregated absorbance response in the presence of various nitro aromatic compounds e.g. DNT, nitro benzene (NB), nitro phenol (NP) and other environmentally relevant metal ions. Our result shows excellent selectivity over other nitro compounds, alkaline, alkaline earth (Li^+, Na^+, K^+, Mg^{2+}, Ca^{2+}) and transition heavy metal ions (Pb^{2+}, Pb^+, Mn^{2+}, Fe^{2+}, Cu^{2+}, Ni^{2+}, Zn^{2+}, Cd^{2+}). So our experimental results clearly demonstrate that our SERS probe can be used for the detection of TNT from environmental sample.

To evaluate the sensitivity of our SERS probe, different concentrations of TNT from one stock solution were evaluated. As shown in Figure 5, the SERS intensity at 1360 cm^{-1} due to

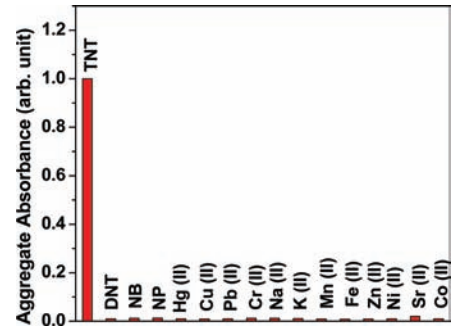

Figure 5. Demonstrating selectivity of our SERS probe over other nitro aromatic compounds and heavy metal ions. It shows how the aggregate absorbance varies with the addition TNT (500×10^{-9} M) and other impurities (50×10^{-6} M).

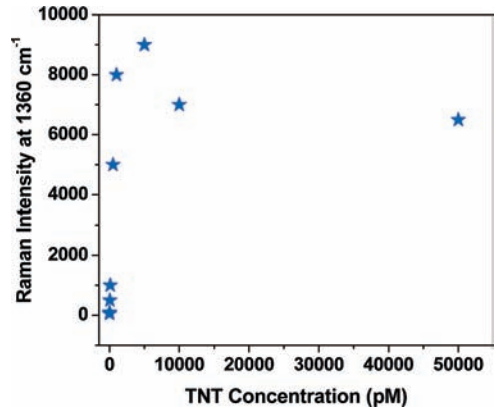

Figure 6. Plot demonstrating how Raman intensity at 1360 cm^{-1} changes upon addition of different concentration of TNT.

NO_2 symmetric stretching vibration is highly sensitive to the concentration of TNT. Our experimental results (as shown in Figure 6) clearly demonstrate that the detection capability of our SERS probe is as low as 2 pM TNT. To the best of our knowledge, the detection limit achieved with our SERS probe, represents the lowest among the reported methods. Our experimental results also show that as we increase the concentration of TNT above 10 nM, the SERS intensity starts decreasing. At extremely low concentration, the surface coverage by TNT is submonolayer and in the absence of sufficient scattering molecules the SERS signal is weak. With increasing concentration, as the surface coverage increases, the SERS intensity increases and attains maximum intensity at monolayer coverage. With further increase in concentration of the adsorbates, multiple layers are formed and SERS signal decreases in intensity. It may be due to the fact that as we increase the concentration of TNT, aggregates or cluster size increases. Since it is known that small cluster is better for hot spot formation, increasing cluster size may decrease the number of hot spots and as a result, intensity decreases after certain concentration of TNT.

Conclusion

In conclusion, in this article, we have demonstrated for the first time a label-free, highly selective and ultra sensitive SERS probe TNT recognition in 2 pM level in aqueous solution. We have shown that due to the formation of Meisenheimer complex between TNT and cysteine, gold nanoparticles undergo aggregation in the presence of TNT via electrostatic interaction between Meisenheimer complex bound gold nanoparticle and cysteine modified gold nanoparticle. As a result, it formed

several hot spots and provided a significant enhancement of the Raman signal intensity by 9 orders of magnitude through electromagnetic field enhancements. Our experimental results show that TNT can be detected quickly and accurately without any dye tagging in 2 pM level with excellent discrimination against other nitro aromatic compounds and heavy metals. This SERS assay is rapid and takes less than 10 min from TNT binding to detection and analysis. Our experimental results reported here show a new possibility of rapid, easy and reliable diagnosis of TNT from environmental sample by measuring the TNT SERS intensity. It is probably possible to improve the SERS sensitivity by several orders of magnitudes by choosing proper materials for generating hot spot and using better detection systems. Although we have shown promising advances in SERS assay, we still need a much greater understanding of how to control surface architecture to stabilize and maximize the SERS response.

Acknowledgment. Dr. Ray thanks DOD grant # W 912HZ-06-C-0057, ARO grant # W911NF-06-1-0512 and NSF-PREM grant # DMR-0611539, for their generous funding. We also thank reviewer whose valuable suggestions improved the quality of the manuscript.

JA905134D